Numerical evaluation of a propane cooling unit for transportable insulated boxes equipped with eutectic tube TES

Francesco FABRIS*[(a)], Silvia MINETTO[(a)], Sergio MARINETTI[(a)], Antonio ROSSETTI[(a)]

(a) National Research Council, Construction Technologies Institute (CNR-ITC)

Padova, 35127, Italy

fabris@itc.cnr.it (*corresponding author), minetto@itc.cnr.it, marinetti@itc.cnr.it, rossetti@itc.cnr.it

ABSTRACT

Traditionally, Cold TES (CTES) has been used in transport refrigeration in the form of eutectic plates mounted inside insulated boxes, especially for last-mile deliveries. Due to their flexibility, these boxes represent a valid option to increase the resilience of the cold chain under emergency situations, like floods, landslides, etc that are becoming more frequent.

To increase the overall sustainability of the entire solution, and to guarantee the accessibility to cheap and widespread refrigerants, this study presents and numerically evaluates the performance of an efficient cooling unit relying on an innovative TES configuration (eutectic tubes) and on natural refrigerant (propane), to replace a baseline cooling unit employing a synthetic refrigerant.

The numerical model is validated against experimental data measured on the baseline unit and demonstrates a +12.6% pulldown COP increase of the proposed system compared to baseline under standard test conditions. Considerations regarding propane charge are also included.

Keywords: Refrigerated transport; Last-mile delivery; Thermal energy storage; Eutectic tubes; Propane.

1 INTRODUCTION

Refrigeration and cold chain systems have become increasingly vital due to their role in food preservation, medicine storage, and industrial applications. The growing global demand for cooling, driven by population growth, urbanization, and climate change, has underscored the need for efficient and sustainable refrigeration technologies. However, this increasing reliance on cooling systems has also led to significant environmental concerns, as the sector is responsible for substantial greenhouse gas (GHG) emissions. In fact, it has been reported by UNEP and FAO (2022) that the cold chain is responsible for almost 4% of global GHG emissions. These emissions arise from both direct refrigerant leaks and indirect emissions related to energy consumption of cooling systems. Addressing these challenges is crucial to achieving environmental sustainability while ensuring the continued functionality of refrigeration-dependent sectors.

Within the cold chain, transport refrigeration represents one of its most environmentally impactful steps, being responsible for nearly 25% of the total cold chain emissions (IIR, 2021). The post-COVID era has witnessed a significant increase in new services related to e-commerce and last-mile delivery of perishable goods (Yang et al., 2021). Consequently, there has been a growing interest in the application of thermal energy storage (TES) solutions in transport refrigeration. Comprehensive reviews on the state-of-the-art utilization of phase change materials (PCMs) for temperature-controlled transport and cold chain distribution are available in Calati et al. (2022) and Umate and Sawarkar (2024). These studies attest that eutectic plates represent the most mature technology based on TES for transportable appliances. Such systems rely on a cooling unit powered by grid electricity to freeze the eutectic plates installed inside the insulated body to be transported, to then exploit the stored energy at low temperature providing passive refrigeration inside the insulated body during transportation. The refrigeration unit is sometimes integrated in the system while in some other designs the plates are connected to a stationary unit and frozen before each delivery mission.

The transition from synthetic refrigerants, such as hydrofluorocarbons (HFCs) and hydrofluoroolefins (HFOs), to natural refrigerants, including ammonia, carbon dioxide, and hydrocarbons, has become a crucial step to be progressively taken to achieve long-term environmental sustainability of refrigeration systems, including transportable units intended for last-mile delivery or for non-stationary applications. The design of efficient units working with natural refrigerants must consider adaptation to overall increase in ambient temperatures and heat waves, which are becoming more and more frequent.

To address the multiple challenges of short distance delivery, this study focuses on the numerical development and performance evaluation of an efficient refrigeration system relying on the simultaneous employment of TES (eutectic tubes) and of a natural refrigerant (propane), serving a small insulated box for preservation of temperature sensitive goods, to replace a baseline cooling unit employing a synthetic refrigerant (R452A), representative of present market solutions.

This design can be a valuable solution in the cold chain as it allows for a more flexible fleet management, as the refrigerated box can be transported by non-specialized trucks, and in conjunction with non-temperature sensitive goods or other similar boxes according to the need. Furthermore, it can operate as temporary storage, after the transport, under critical situations, even at high ambient temperature, being capable of operating off-grid, thanks to TES.

2 THE REFRIGERATION SYSTEM

This study focuses on a transportable insulated box equipped with eutectic tubes, acting as thermal energy storage, for last mile delivery of frozen food products or for emergency response scenarios. A compact refrigeration unit serves the insulated box, both to charge the TES and to decrease the internal air temperature to the setpoint before deliveries.

The insulated box has external dimensions of 1.70 m × 1.00 m × 1.75 m and an internal volume of 1.86 m^3, and it is shown in Figure 1. Each wall of the box consists of a three-layer structure, comprising a 94 mm polyurethane foam core enclosed between two 3 mm glassfiber-reinforced plastic (GRP) layers. To enhance structural rigidity, the box is reinforced with wooden and metallic components. The global heat transfer coefficient of the insulated box, determined in accordance with Annex 1 of the ATP agreement (United Nations, 2024), is K = 0.31 W m^{-2} K^{-1}. The cooling unit is positioned on the left side of the box roof.

Figure 1. Insulated box and attached cooling unit.

In current market, eutectic plates represent an established technology and are regarded as the most mature TES-based solution in cold chain transport applications (Calati et al., 2022), such as for insulated boxes as the one considered for this study. Eutectic plates consist of two cold-formed steel shells containing the refrigerant coils immersed in PCM solution and are generally mounted on the internal walls of the insulated box, acting as TES for the box during deliveries. The refrigeration unit is normally switched off after freezing the plates and the cooling power is provided by PCM melting.

In this study, eutectic tubes are used in place of standard eutectic plates. Eutectic tubes, which are displayed in Figure 2, offer an alternative solution to eutectic plates and present some functional advantages. Firstly, in eutectic tubes the refrigerant pipe is external to the aluminium case containing the PCM. This allows to have a closed and separate circuit for the refrigerant, without any connection; pipe diameter and thickness can be selected to handle potential higher pressures. In addition, the use of an external refrigerant pipe allows simultaneous heat transfer with the PCM and with the air inside the insulated box, leading to a quicker temperature decrease inside the box during pulldown. Secondly, thanks to their modular design and structure, eutectic tubes can be stacked together in case of higher thermal loads. Lastly, the aluminium case containing the PCM can be easily opened unscrewing the front plate displayed in Figure 2a, allowing in-house PCM filling and potential swaps of the PCM solution according to the temperature levels required for the correct preservation and transport of different products.

In this application, seven eutectic tubes are mounted inside the box on the top wall and connected in series, as it can be observed in Figure 2b. Each eutectic tube is 1.2 m long and is charged with 5.16 kg of PCM. The PCM, a eutectic solution based on inorganic salts, is characterized by a latent heat of fusion equal to 243 kJ kg^{-1} and the nominal phase change temperature declared by the manufacturer is equal to -33.5 °C (Diversey, 2019). Therefore, the maximum energy that can be stored by the seven eutectic tubes is 8.8 MJ.

(a) (b)

Figure 2. Eutectic tubes: (a) front view detail; (b) complete tubes setup inside the insulated box.

During the pulldown, the eutectic tubes are frozen by the refrigeration unit, powered by grid electricity. When the pulldown process starts, the PCM stored inside the tubes is cooled down and eventually solidifies at the selected temperature level. This step corresponds to the PCM “charging” phase, i.e. storage of energy. At the end of the pulldown, the cooling unit is turned off and the insulated box is loaded with the goods to be transported. During delivery missions, the insulated box is transported by the vehicle and the required temperature for preservation is maintained as the heat infiltrating the box is absorbed in the eutectic plates, where the PCM progressively melts at fixed temperature level, granting a passive refrigeration effect inside the insulated box without turning on the cooling unit. This phase corresponds to the “discharging” phase of the PCM. Compared to a traditional vapour compression cooling unit, the eutectic tubes solution can provide benefits in terms of noise, local pollution, efficiency and emissions linked to primary energy consumption.

The baseline cooling unit currently employed consists of a direct expansion vapor compression unit, whose simplified schematic is presented in Figure 3, working with synthetic refrigerant R452A. The eutectic tubes correspond to the evaporator of the cooling unit. The unit operates with fixed compressor speed. A

thermostatic expansion valve controls the refrigerant evaporation pressure to achieve a fixed superheat (5 K) at the evaporator exit.

To increase the overall sustainability for this application, the replacement of the synthetic refrigerant R452A with the natural refrigerant R290 (propane) is considered in this study. Since R290 is a highly flammable refrigerant (safety class A3), charge reduction represents the major challenge for its applicability. For this reason, while maintain the overall schematic of Figure 3, the liquid receiver is removed from the R290 unit. The refrigerant circuit is therefore critically charged, as it will be further discussed in the Section 4. Also in this case, the unit operates with fixed speed compressor, and a thermostatic expansion valve enforces a 5 K superheat at the evaporator exit.

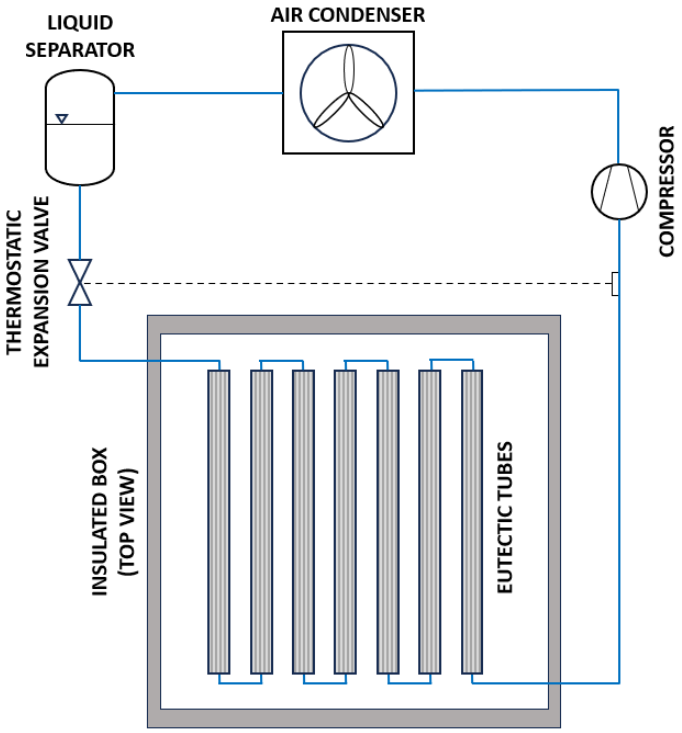

Figure 3. Refrigeration system simplified schematic.

3 NUMERICAL MODEL

The refrigeration system is dynamically modelled using the commercial multi-physics software Simcenter Amesim (Siemens, 2025). The model employs a lumped-parameters approach, wherein real components are discretized into interconnected elements to represent the entire system. Each element is governed by nonlinear time-dependent differential equations that define the state variables. These equations are assembled into a system of differential equations, which is subsequently integrated over time to simulate the system's dynamic behaviour.

This numerical approach has been extensively detailed in previous works by the same authors (Artuso et al., 2020; Fabris et al., 2021). A concise description of the system components included in the model, the numerical discretization and underlying assumptions, as well as the empirical correlations utilized to evaluate heat transfer processes, is provided below.

A fixed displacement compressor model is implemented, with volumetric and compression efficiencies interpolated as functions of the pressure ratio and suction pressure from manufacturer data for the R452A and R290 compressors. The R290 compressor was selected from manufacturer's catalogue with capacity as close as possible to the reference R452A one; all the other components remain the same for the R290 and R452A systems.

The fin-and-tube condenser is discretized into N = 4 lumped volumes. Each volume is further subdivided into three nodes, corresponding to the refrigerant flow, the tube wall and fins, and the surrounding air. The geometric characteristics of the heat exchanger, such as area and mass, are evenly distributed across the lumped elements. Heat transfer processes account for internal convection between the refrigerant and the internal wall, conduction through the wall and fins, and external convection between the fins and ambient air.

Each of the seven eutectic tubes is discretized into N = 5 lumped volumes. Each discretized volume considers the overall heat fluxes between the refrigerant, the eutectic tube, the PCM and the insulated box, according to the discretization schematic presented in Figure 4. Also in this case, the geometric characteristics are equally distributed. Internal convection between refrigerant and copper pipe, conduction between the refrigerant copper pipe and the eutectic tube aluminium case, conduction through PCM, external convection between the tube aluminium case and air inside the insulated box, and radiation between the tube aluminium case and the internal walls of the box are considered. Moreover, heat transfer along consecutive discretized elements of refrigerant, copper, aluminium and PCM is also considered. The PCM behaviour is described by providing its main thermophysical properties (density and specific heat of liquid and solid phases, thermal conductivity, latent heat of fusion and temperature of phase change) as an input of the model.

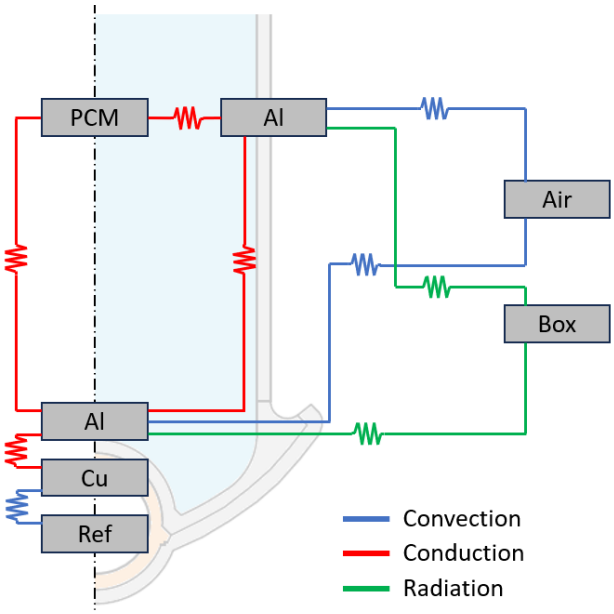

Figure 4. Discretization schematic of each eutectic tube lumped volume. Ref: refrigerant; CU: copper pipe; Al: aluminium case; PCM: phase change material; Air: insulated box internal air; Box: insulated box internal walls.

Convective heat transfer coefficients are determined using empirical correlations from the literature. For refrigerant-side elements, the Gnielinski correlation (1976) is applied for single-phase flow, the Shah correlation (1979) for two-phase condensation, and the VDI correlation in horizontal tubes (Steiner and Taborek, 1992) for two-phase boiling. For air-side elements within the condenser, the Colburn J-factor correlation (McQuiston, 1978) is employed. Additionally, heat exchange between the external surface of the eutectic tubes and the surrounding air is evaluated using the Churchill and Chu (1975) correlation for natural convection over a flat plate.

The dynamic response of the insulated box is modelled by discretizing the box walls into a series of 7 thermal capacities and 6 thermal resistances. The thermal capacitances are estimated based on the box's geometrical and material properties, while the thermal resistances incorporate both geometric and material considerations, as well as thermal bridges associated with doors and metallic structural reinforcements. This approach ensures an accurate reproduction of the global heat transfer coefficient measured in the ATP test ($K = 0.31\ W\ m^{-2}\ K^{-1}$).

4 RESULTS AND DISCUSSION

4.1 Baseline unit experimental setup

The baseline R452A system has been experimentally tested to assess its thermodynamic and energy performance under nominal operating conditions. In particular, the experimental test is based on the ATP test procedure defined for eutectic plates equipment, as described in Annex 1 of the ATP itself (United Nations, 2024).

The test is conducted at T_{amb} approximately constant and with a mean value equal to 28.8 °C over the 32-hours test duration, with standard deviation equal to σ = 0.9 °C. Once the mean inside temperature of the insulated box and the temperature of the eutectic tubes are in equilibrium with the environmental temperature, the doors are closed, and the cooling unit is turned on. The insulated box is kept closed with the cooling unit in operation for 24 hours, to freeze the PCM contained inside the eutectic tubes. After 24 hours, the cooling unit is turned off. The objective of the test is to assess how long the mean temperature inside the insulated box stays below $T_{i,threshold}$ = -20 °C, after switching off the cooling unit.

Several thermocouples are placed in key points of the refrigeration system, to assess the thermodynamic cycle and the air and tubes temperatures, and the temperature values are logged through an Agilent 34970A Data Acquisition Unit equipped with two Agilent 34901A multiplexer modules. The main electrical parameters (power consumption, voltage, current, frequency and power factor) are logged through a high precision multimeter. The list of the equipment used for data acquisition, their accuracy and the sampling rate is reported in Table 1.

Table 1. List of the equipment used for data acquisition and their accuracy.

Type	Instrument	Placement	Accuracy	Sampling rate
Temperature sensors	T-type thermocouples	Compressor suction and discharge, condenser outlet, inlet and surface of eutectic tubes, tubes outlet, internal and external air	± 1.0 °C	1/60 Hz
Electrical parameters	HT Instruments PQA 824	System electrical utilities (compressor + condenser fan)	± 0.5 % (Voltage) ± 0.5 % (Current) ± 1.0 % (Power)	1/120 Hz

The ambient temperature (T_{amb}), the air temperature inside the insulated box (T_i) and the refrigerant evaporation temperature (T_{ev}) over the 32 hours of the complete experimental test are presented in Figure 5. The test assesses that the energy stored in the eutectic plates during the 24 hours pulldown is sufficient to guarantee an almost 8 hours autonomy below the internal air temperature setpoint of -20 °C with fixed external temperature conditions, ensuring compliance with ATP prescriptions.

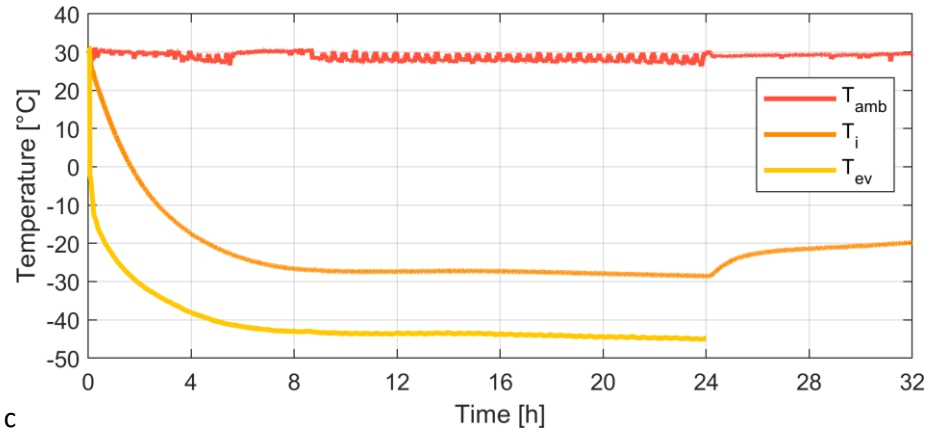

c

Figure 5. Experimental test on baseline R452A system.

4.2 Numerical model validation

A numerical model of the baseline R452A system is developed following the approach presented in Section 3, with the objective of comparing the simulated cooling system performance to the experimental performance. In the simulations, the complete 32-hours test is considered. The ambient temperature profile registered during the experimental test presented in Section 4.1 is used as the input of the numerical simulation, to evaluate the unit under the same operating conditions occurred during the experiment.

As previously described in Section 3, the thermophysical properties of the PCM represent an input of the model. According to the data reported in the commercial datasheet of the eutectic material (Diversey, 2019), the PCM is commercially labelled as having a phase change temperature of -33.5 °C. However, since several studies in literature report that the actual solidification temperature of a PCM might present significant differences from the nominal value due to bad nucleation reasons and to the supercooling phenomenon (Huang et al., 2010; Gunther et al., 2011; Tan et al., 2020), and that the solidification (during PCM "charge") and melting (during PCM "discharge") can occur at different temperatures due to the PCM hysteresis phenomenon (Klimes et al., 2020; Liu et al., 2020), the phase change temperatures have been best fitted by means of a preliminary sensitivity analysis.

Firstly, the first 24-hours pulldown are considered, to determine the best fit of the PCM solidification temperature during its charging phase. The solidification temperature (T_{sol}) is varied between -33 °C and -36 °C. The root mean square error (RMSE) on the internal air temperature (T_i), normalized on the experimentally measured range of variation of T_i, is calculated as defined in Eq. (1), where t_0 and t_{END} represent hour 0 and hour 24 of the experimental test. Similarly, the RMSE on the electrical power consumption (P), normalized on the mean value of the experimentally measured P, is calculated as defined in Eq. (2). The sum of these two normalized RMSE, calculated as described in Eq. (3), has been used as fitness function in the best fit.

$$RMSE_{Ti} = \frac{\sqrt{\frac{\sum_{t=t_0}^{t_{END}} (T_{i,exp}^{t} - T_{i,sim}^{t})^2}{(t_{END} - t_0)}}}{(T_{i,exp,max} - T_{i,exp,min})} \quad (1)$$

$$RMSE_{P} = \frac{\sqrt{\frac{\sum_{t=t_0}^{t_{END}} (P_{exp}^{t} - P_{sim}^{t})^2}{(t_{END} - t_0)}}}{\bar{P}_{exp}} \quad (2)$$

$$RMSE_{TOT} = RMSE_{Ti} + RMSE_{P} \quad (3)$$

Results are presented in Table 2. The sensitivity analysis shows that the best fit of the numerical model on experimental data during the PCM charging phase is achieved with T_{sol} = -35 °C.

Table 2. Normalized RMSE of the numerical model during PCM charging phase (hours 0-24) as a function of the PCM solidification temperature.

T_{sol} [°C]	$RMSE_{Ti}$ [-]	$RMSE_P$ [-]	$RMSE_{TOT}$ [-]
-33	0.0186	0.0349	0.0534
-34	0.0129	0.0336	0.0465
-35	0.0124	0.0323	0.0448
-36	0.0166	0.0294	0.0459

The melting temperature (T_{melt}) is obtained applying a similar procedure to the discharging phase. T_{melt} is varied between -31 °C and -34 °C. For the discharging phase, the model accuracy is assessed using only the $RMSE_{Ti}$ defined in Eq. (1). In this case, t_0 and t_{END} represent hour 24 and hour 32 of the experimental test. Results are reported in Table 3, showing that the best fit is achieved with T_{melt} = -32 °C.

The solidification and melting temperature obtained (T_{sol} = -35 °C, T_{melt} = -32 °C) are coherent with the nominal manufacturer phase change temperature of -33.5 °C and the hysteresis seems in line with the literature for these materials.

Table 3. Normalized RMSE of the numerical model during PCM charging phase (hours 24-32) as a function of the PCM melting temperature.

T_{melt} [°C]	$RMSE_{Ti}$ [-]
-31	0.0970
-32	0.0576
-33	0.0955
-34	0.1251

Figure 6 presents a comparison of the numerical model with experimental data. The simulated total electrical energy consumption over the 24 hours of the pulldown ($E_{TOT,sim}$ = 51.9 MJ) is then compared to the experimentally measured electrical consumption ($E_{TOT,exp}$ = 51.5 MJ), showing a difference between the numerical model and the experimental data equal to +0.8%.

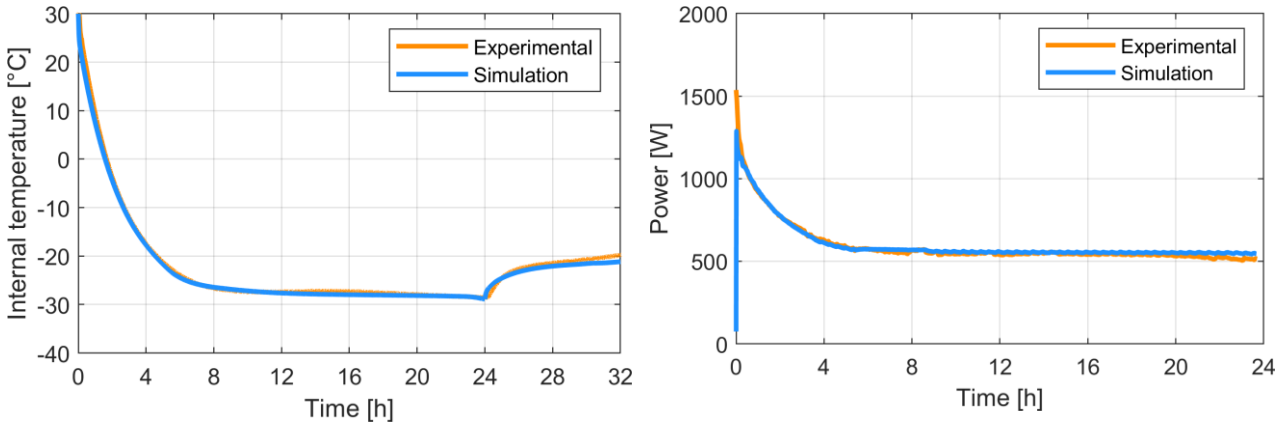

(a) (b)

Figure 6. Performance test on baseline R452A system: (a) experimental and numerical internal air temperature inside the insulated box; (b) Experimental and numerical electrical power input.

4.3 Numerical evaluation of R290 unit

Once the numerical approach is validated against the experimental data, the same approach is used for the proposed R290 system. To allow a clear comparison between the proposed system and the baseline one, the same test described in Section 4.2 is used for the numerical simulations. The nominal ambient temperature

of 30 °C is set as constant boundary for the whole duration of the test as well as for the isothermal initialization of the model thermal inertia. Results are presented in Figure 7.

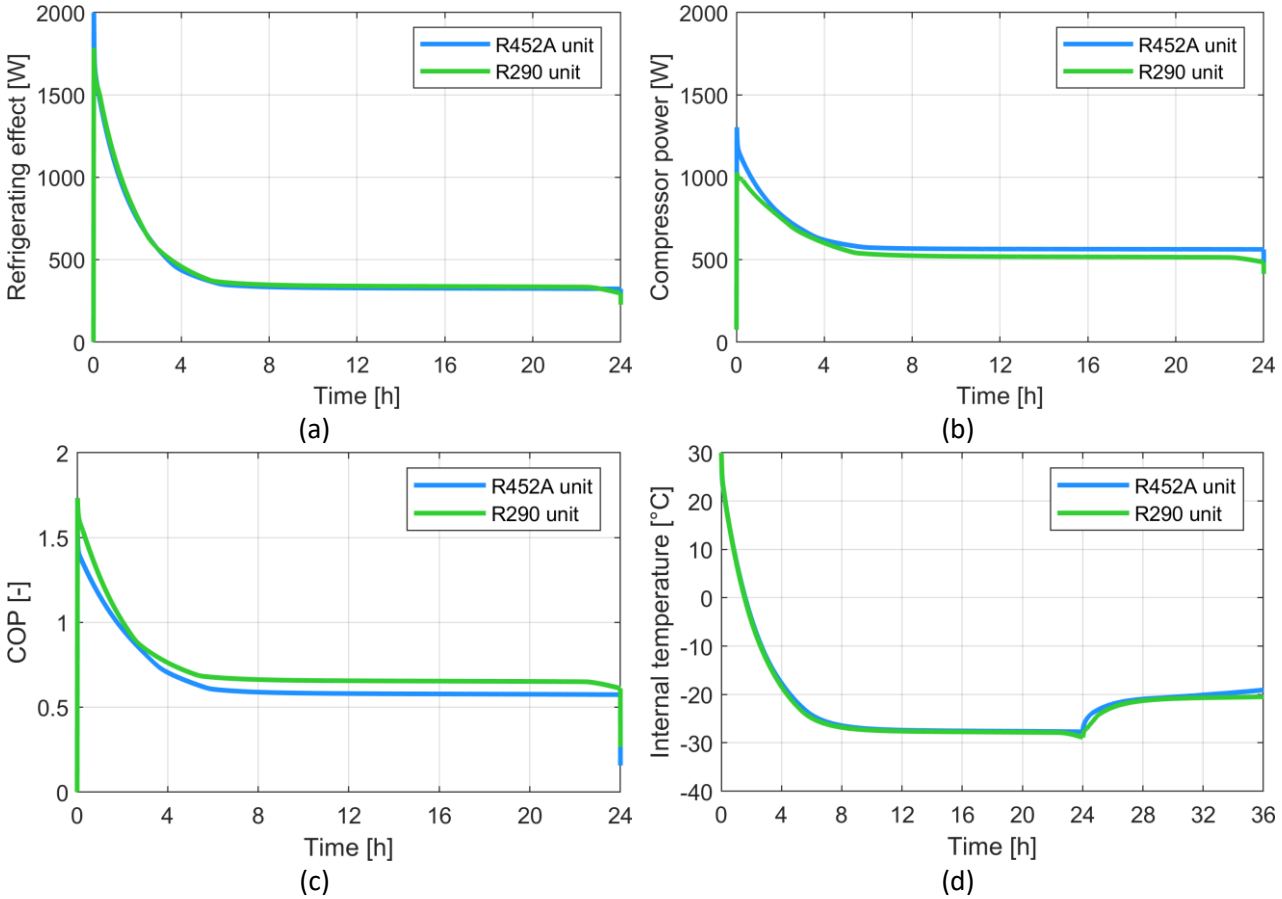

Figure 7. Performance comparison between baseline R452A system and R290 system: (a) COP; (b) refrigerating effect; (c) compressor power; (d) air temperature inside the box.

The R290 system presents a better performance compared to the baseline R452A system along the pulldown. In fact, while the energy provided by the R290 cooling unit in the 24 hours (36.7 MJ) is slightly higher (+4.6%) than the one provided by the R452A unit (35.1 MJ), there is a significant decrease of the compressor power input for the case of the R290 unit along the whole duration of the simulation. In fact, the total energy consumption in the 24 hours is equal to 55.8 MJ for the R452A unit and to 51.9 MJ for the R290 unit, with an energy consumption reduction equal to -7.1%. As a result, the overall pulldown COP, defined as the ratio between the total cooling energy provided by the unit and the total electrical energy consumption of the unit during the 24-hours pulldown, is equal to 0.63 for the R452A baseline system and to 0.71 (+12.6%) for the R290 system.

Furthermore, the additional cooling energy provided by the R290 unit during the pulldown results both in an increased energy stored in the TES and in a decrease of the temperature of the insulated box mass itself compared to the R452A system. As an overall result, there is a higher thermal inertia of the PCM and of the box, leading to an increase of the time in which the air inside the box is maintained below the threshold of -20 °C after the end of the pulldown (where the ambient temperature is still kept constant at 30 °C). This difference might significantly affect the time period after which the cooling unit has to be switched on again, especially when the temperature threshold must be strictly respected due to regulations on perishable goods preservation conditions.

4.4 R290 charge evaluation

Finally, as anticipated in Section 2, the minimization of refrigerant charge is a critical requirement to guarantee safety of vapor compression systems employing hydrocarbons, such as propane, as operating fluids.

The used numerical approach accounts for the internal volumes of each subcomponent in the numerical scheme and dynamically resolves the mass of refrigerant contained, according to the operating condition of the system. The total refrigerant charge is given as an input to the model. For the R290 unit simulation described in Section 4.3, the charge is set to 130 g. At the end of the 24-hours pulldown the charge is distributed as follows: 100 g of propane in the condenser coils, 26 g in the connection pipes between the compressor, condenser and eutectic pipes and only 4 g in the refrigerant coils attached to the eutectic tubes inside the insulated box.

Moreover, since the system is critically charged, the effect of the variation of R290 charge in the circuit on the performance of the cooling unit is evaluated. Steady-state numerical simulations are performed in which a fixed heat source is set at -35 °C, to represent the unit design operating conditions (corresponding to the PCM solidification temperature), and variable ambient temperature (between 15 °C and 55 °C) and R290 charge (between 50 g and 150 g) are considered. The variation of the unit cooling effect depending on the simulated conditions is presented in Figure 8.

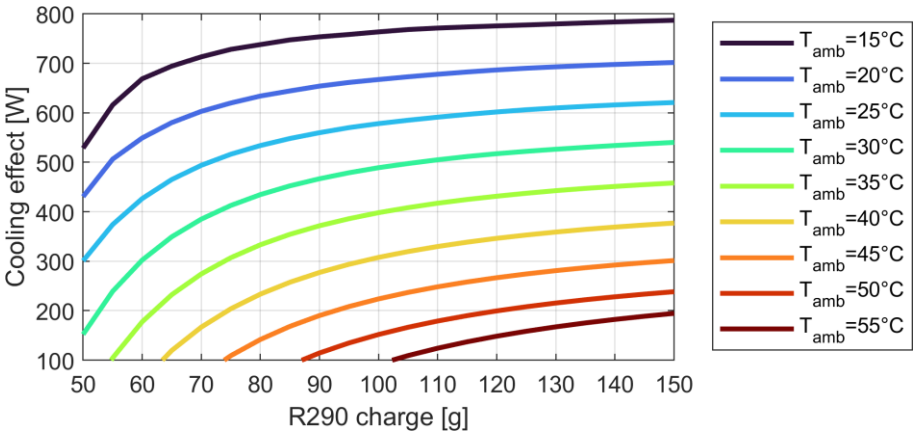

Figure 8. Steady-state cooling effect of the R290 unit as a function of ambient temperature and R290 charge, with fixed heat source at -35 °C.

The unit cooling effect is strongly influenced by the refrigerant charge, especially when the refrigerant charge is too low for the system. In fact, in the range of R290 charge below 100 g, a small reduction of the charge determines a significant drop in cooling effect which, for a specific ambient temperature, can result in an insufficient cooling energy provided to the eutectic tubes and, consequently, stored in the TES during a fixed duration pulldown, causing substantial decrease in the time autonomy of the insulated box below the temperature threshold. On the contrary, with R290 charge above 130 g, the variation of cooling effect with charge progressively decreases, with the only exception of extremely high ambient temperatures (above 45 °C).

While some important phenomena as the refrigerant solubility in the lubricant are neglected in the numerical simulations, these results suggests that such cooling unit could be realized with a total charge of R290 under 150 g, presenting good performance even with considerably hot ambient temperatures (up to 40-45 °C).

5 CONCLUSIONS

In this study, an efficient system based on an innovative TES configuration (eutectic tubes in place of traditional eutectic plates) and employing the natural refrigerants propane (R290) in the attached cooling unit is proposed as an energy efficient and environmentally sustainable solution for transportable insulated

boxes applications, which can be employed in standard last-mile deliveries of food as well as to increase the flexibility and resilience of the cold chain in emergency situations. The proposed propane unit is meant to replace a baseline system employing the synthetic refrigerant R452A.

The performance of the baseline R452A system is experimentally assessed in standard test conditions based on the ATP test procedure on class C eutectic plates equipment, consisting in a 24-hours pulldown (PCM charging phase), followed by 8 hours with the cooling unit turned off, with ambient temperature kept constant at approximately 30 °C. A dynamic numerical model of the baseline and of the proposed refrigeration systems is developed. The PCM phase change temperatures in the numerical model are assessed through a preliminary sensitivity analysis. The numerical model is validated against the experimental data, showing good accordance on the dynamic evolution of internal air temperature and power consumption and achieving a +0.8% error on the total energy consumption.

The validated numerical approach is then used to simulate the same pulldown test conditions for the proposed R290 unit, using only propane as an almost drop-in for the R452A refrigerant. The R290 system outperforms the baseline R452A system, achieving a +4.6% increase in cooling energy provided by the unit, a -7.1% decrease in total energy consumption and an overall +12.6% increase in pulldown COP over the 24-hours test. Moreover, the extra cooling energy delivered by the unit and stored in the TES allows to increase the time in which the air temperature inside the box is maintained below the threshold temperature (-20 °C) with the cooling unit turned off. The proposed R290 unit operates with a very limited charge, equal to 130 g. Overall, the numerical results suggest that the proposed R290 unit can contribute to increase the sustainability of small transportable cooling systems by replacing currently employed synthetic refrigerants-based solutions, while at the same time minimizing potential issues linked to use of hydrocarbons in mobile applications. The presented solution can provide a valuable mean of transportation and temporary storage under critical situations, even at high ambient temperature, being capable of operating off-grid, thanks to TES, thus contributing to the resilience of the cold chain.

ACKNOWLEDGEMENTS

The activity described in this manuscript has been performed within the project ENOUGH, which has received funding from the European Union's Horizon 2020 research and innovation programme under grant agreement No 101036588.

The Authors would like to thank the industrial partner Eutectic System S.r.l. for the collaboration and support to this study.

REFERENCES

Artuso, P., Marinetti, S., Minetto, S., Del Col, D., Rossetti, A. (2020). Modelling the performance of a new cooling unit for refrigerated transport using carbon dioxide as the refrigerant. International Journal of Refrigeration 115, 158–171. https://doi.org/10.1016/j.ijrefrig.2020.02.032

Calati, M., Zilio, C., Righetti, G., Longo, G., Hooman, K., Mancin, S. (2022). Latent thermal energy storage for refrigerated trucks. International Journal of Refrigeration 136, 124-133. https://doi.org/10.1016/j.ijrefrig.2022.01.018

Churchill, S. W., Chu, H. H. S. (1975). Correlating equations for laminar and turbulent free convection from a vertical plate. International Journal of Heat and Mass Transfer 18, 1323-1329. https://doi.org/10.1016/0017-9310(75)90243-4

Diversey (2019). Hoesch E 33 Spezial Product Information Sheet. Available online: https://solenis.my.salesforce.com/sfc/p/#50000000JWVF/a/UX000003kFnA/4NsDmgvfPckQKrx8Kzwfc3DTVbQ02.BSLOkFVMvnMQc

Fabris, F., Artuso, P., Marinetti, S., Minetto, S., Rossetti, A. (2021). Dynamic modelling of a CO2 transport refrigeration unit with multiple configurations. Applied Thermal Engineering 189 (February), 116749. https://doi.org/10.1016/j.applthermaleng.2021.116749

Fabris, F., Marinetti, S., Minetto, S., Rossetti, A. (2024). Numerical characterization of a propane-CO2

refrigeration system developed for TES last-mile delivery. 8th IIR International Conference on Sustainability and the Cold Chain, June 9-11 2024, Tokyo, Japan. http://dx.doi.org/10.18462/iir.iccc2024.1090

Gnielinski, V. (1976). New equations for heat and mass transfer in turbulent pipe and channel flow. International Chemical Engineering 16, 359-368.

Gunther, E., Huang, L., Mehling, H., Doetsch, C. (2011). Subcooling in PCM emulsions – Part 2: Interpretation in terms of nucleation theory. Thermochimica Acta 522, 199-204. https://doi.org/10.1016/j.tca.2011.04.027

Huang, L., Gunther, E., Doetsch, C., Mehling, H. (2010). Subcooling in PCM emulsions – Part 1: Experimental. Thermochimica Acta 509, 93-99. https://doi.org/10.1016/j.tca.2010.06.006

International Institute of Refrigeration (IIR) (2021). 7th informatory note on refrigeration and food. The Carbon Footprint of the Cold Chain. https://doi.org/10.18462/iir.INfood07.04.2021

Klimeš, L., Charvát, P., Mastani Joybari, M., Zálešák, M., Haghighat, F., Panchabikesan, K., El Mankibi, M., Yuan, Y. (2020). Computer modelling and experimental investigation of phase change hysteresis of PCMs: The state-of-the-art review. Applied Energy, 263, 114572. https://doi.org/10.1016/j.apenergy.2020.114572

Liu, L., Zhang, X., Xu, X., Zhao, Y., Zhang, S. (2020). The research progress on phase change hysteresis affecting the thermal characteristics of PCMs: A review. Journal of Molecular Liquids, 317, 113760. https://doi.org/10.1016/j.molliq.2020.113760

McQuiston, F. (1978). Correlation of heat, mass and momentum transport coefficients for plate-fin-tube heat transfer surfaces with staggered tubes. ASHRAE Transaction 84 (1), 294-309.

Shah, M. (1979). A general correlation for heat transfer during film condensation inside pipes. International Journal of Heat and Mass Transfer 22, 547-556. https://doi.org/10.1016/0017-9310(79)90058-9

Siemens (2025). Simcenter system simulation - Simcenter Amesim software. Available online: https://plm.sw.siemens.com/en-US/simcenter/systems-simulation/amesim/

Steiner, D., Taborek, J. (1992). Flow boiling heat transfer in vertical tubes correlated by an asymptotic model. Heat Transfer Engineering 13, 322-329. https://doi.org/10.1080/01457639208939774

Tan, P., Lindberg, P., Eichler, K., Loveryd, P., Johansson, P., Sasic Kalagasidis, A. (2020). Effect of phase separation and supercooling on the storage capacity in a commercial latent heat thermal energy storage: Experimental cycling of a salt hydrate PCM. Journal of Energy Storage 29, 101266. https://doi.org/10.1016/j.est.2020.101266

Umate, T. B., Sawarkar, P. D. (2024). A review on thermal energy storage using phase change materials for refrigerated trucks: Active and passive approaches. Journal of Energy Storage 75, 109704. https://doi.org/10.1016/j.est.2023.109704

UNEP and FAO (2022). Sustainable food cold chains: Opportunities, challenges and the way forward. Nairobi, UNEP and Rome, FAO. https://doi.org/10.4060/cc0923en

United Nations (2024). Agreement on the International Carriage of Perishable Food-stuffs and on the Special Equipment to be Used for Such Carriage (ATP). UNECE Transport Division, Geneva, Switzerland, 2024. Available: https://unece.org/text-and-status-agreement

Yang, Z., Tate, J.E., Morganti, E., Shepherd, S.P. (2021). Real-world CO2 and NOX emissions from refrigerated vans. Sci. Total Environ. 763, 142974. https://doi.org/10.1016/j.scitotenv.2020.142974